



PARP-14 Promotes Survival of Mammalian α but Not β Pancreatic Cells Following Cytokine Treatment

Floriana D'Angeli¹, Marina Scalia², Matilde Cirnigliaro², Cristina Satriano³,
Vincenza Barresi¹, Nicolò Musso¹, Angela Trovato-Salinaro¹, Davide Barbagallo²,
Marco Ragusa², Cinzia Di Pietro², Michele Purrello² and Vittoria Spina-Purrello^{1*}

¹ Department of Biomedical and Biotechnological Sciences, Section of Medical Biochemistry, University of Catania, Catania, Italy, ² Department of Biomedical and Biotechnological Sciences, Section of Biology and Genetics, University of Catania, Catania, Italy, ³ Department of Chemical Sciences, University of Catania, Catania, Italy

OPEN ACCESS

Edited by:

Marco Falasca,
Curtin University, Australia

Reviewed by:

Marta Letizia Hribal,
Università degli studi Magna Græcia di
Catanzaro, Italy
Giulia Cantini,
University of Florence, Italy

*Correspondence:

Vittoria Spina-Purrello
spinavit@unict.it

Specialty section:

This article was submitted to
Cellular Endocrinology,
a section of the journal
Frontiers in Endocrinology

Received: 31 January 2019

Accepted: 12 April 2019

Published: 03 May 2019

Citation:

D'Angeli F, Scalia M, Cirnigliaro M,
Satriano C, Barresi V, Musso N,
Trovato-Salinaro A, Barbagallo D,
Ragusa M, Di Pietro C, Purrello M and
Spina-Purrello V (2019) PARP-14
Promotes Survival of Mammalian α
but Not β Pancreatic Cells Following
Cytokine Treatment.
Front. Endocrinol. 10:271.
doi: 10.3389/fendo.2019.00271

PARP-14 (poly-ADP Ribose Polymerase-14), a member of the PARP family, belongs to the group of Bal proteins (B Aggressive Lymphoma). PARP-14 has recently appeared to be involved in the transduction pathway mediated by JNKs (c Jun N terminal Kinases), among which JNK2 promotes cancer cell survival. Several pharmacological PARP inhibitors are currently used as antitumor agents, even though they have also proved to be effective in many inflammatory diseases. Cytokine release from immune system cells characterizes many autoimmune inflammatory disorders, including type I diabetes, in which the inflammatory state causes β cell loss. Nevertheless, growing evidence supports a concomitant implication of glucagon secreting α cells in type I diabetes progression. Here, we provide evidence on the activation of a survival pathway, mediated by PARP-14, in pancreatic α cells, following treatment of α TC1.6 glucagonoma and β TC1 insulinoma cell lines with a cytokine cocktail: interleukin 1 beta (IL-1 β), interferon gamma (IFN- γ) and tumor necrosis factor alpha (TNF- α). Through qPCR, western blot and confocal analysis, we demonstrated higher expression levels of PARP-14 in α TC1.6 cells with respect to β TC1 cells under inflammatory stimuli. By cytofluorimetric and caspase-3 assays, we showed the higher resistance of α cells compared to β cells to apoptosis induced by cytokines. Furthermore, the ability of PJ-34 to modulate the expression of the proteins involved in the survival pathway suggests a protective role of PARP-14. These data shed light on a poorly characterized function of PARP-14 in α TC1.6 cells in inflammatory contexts, widening the potential pharmacological applications of PARP inhibitors.

Keywords: PARP-14, JNK1, JNK2, cytokines, PJ-34, survival

INTRODUCTION

Poly(ADP-ribosyl)ation is a well-known post-translational modification of proteins, which uses NAD⁺ as a substrate. It is involved in cell proliferation and survival, DNA repair, inflammation and cell death (1–5). PARP-1 is the most studied member of the PARP super-family, which is comprised of 17 proteins in humans. The PARP family proteins are encoded by different genes, all displaying a conserved catalytic domain containing PAR (poly ADP ribose) (6–11). PARP-1, PARP-2, PARP-5a, and PARP-5b catalyze the polymerization of ADP-ribose units (PARylation) through $\alpha(1 \rightarrow 2)$ O-glycosidic bonds in linear or branched chains (12). PARP mono enzymes, mono-(ADP-ribosyl) transferases (MARTs) (i.e., PARP-3, PARP-4, PARP-6, PARP-10, PARP-14,

PARP-15, and PARP-16) catalyze the addition of a single ADP-ribose unit to target proteins through a process called MARYlation (13). The implication of poly- or mono-(ADP-ribosylation) in many pathological conditions has promoted the development of pharmacological molecules able to block these processes (12, 14). PARP-14, also known as B aggressive lymphoma protein (BAL2 protein) in humans, belongs to macro-PARPs, a branch of the PARP family (15). Recent evidence has highlighted the role of PARP-14 in cancer and in many other diseases (15–20). In multiple myeloma, the involvement of PARP-14 in the JNK pathway has been reported, precisely between JNK2 and JNK1 (16). By binding to JNK1 and inhibiting its pro-apoptotic activity, PARP-14 acts as a pro-survival signal. This inhibition would be responsible for blocking the phosphorylation of downstream proteins such as p53, promoting cell survival (21). In our study, we used mouse α TC1.6 glucagonoma and β TC1 insulinoma cells as experimental models to verify the molecular basis of the involvement of PARP-14 in the JNK pathway in pancreatic inflammatory state. It is well-established that pro-inflammatory cytokines, such as interleukin-1 β (IL-1 β), interferon- γ (IFN γ) and tumor necrosis factor- α (TNF α), are major candidates for causing apoptotic death of pancreatic β cells and immune-mediated diabetes (20, 22–25). Therefore, we set out to investigate the ability of α cells, compared to β cells, to resist cytokines, evaluating the role played in this system by PARP-14, which we found to be overexpressed in α TC1.6 cells. The results obtained, also by using the PARP inhibitor PJ-34, allowed us to confirm that PARP-14 is involved in a transduction pathway mediated by JNKs and plays a protective role by promoting α cell survival.

MATERIALS AND METHODS

Chemicals and Antibodies

Reagent grade chemicals were purchased from Sigma Chemicals Co. (St. Louis, MO, USA) or E. Merck (Darmstadt, Germany, EU). PARP-14 inhibitor PJ-34 [N-(6-Oxo-5,6-dihydrophenanthridin-2-yl)-N,N-dimethylacetamide.HCl] was from Calbiochem. (La Jolla, CA, USA). The primary antibodies against PARP-14 (mouse monoclonal and goat polyclonal antibodies) were from Santa Cruz Biotechnology Inc. (CA, USA); rabbit polyclonal antibody to c Jun N terminal Kinase 1 (JNK1) and rabbit polyclonal antibody to c Jun N terminal Kinase 2 (JNK2) were from ProteintechTM; rabbit polyclonal antibody against phospho-p53 and mouse monoclonal antibody against p53 were purchased from Cell Signaling Technology[®] and mouse monoclonal antibody against Glyceraldehyde 3-phosphate dehydrogenase (GAPDH) was from Abcam. Reagents for qPCR Trizol, deoxyribonuclease 1 (DNase I Amplification Grade), High Capacity RNA-to-cDNA Kit, Power SYBR[®] Green PCR Master Mix, were from LifetechnologiesTM, Foster-City (CA, USA).

Cell Culture and Treatment With Cytokines

Mouse glucagonoma α TC1.6 cells were purchased from the American Type Culture Collection (ATCC). Cells were

maintained in Dulbecco's Modified Eagle Medium (DMEM—Sigma-Aldrich, Saint Louis, MO, USA) containing 10% fetal bovine serum (FBS), 2 mM L-glutamine, 0.15% 4-(2-hydroxyethyl)-1-piperazineethanesulfonic acid (HEPES) 15 mM, 1% non-essential amino acids (NEAA), 0.02% bovine serum albumins (BSA, Sigma-Aldrich), 25 mM d-glucose (Sigma-Aldrich), 100 U/ml penicillin, and 100 μ g/ml streptomycin, at 37°C, with 5%-CO₂ humidified incubator. Mouse insulinoma β TC1 cells were also from ATCC; cells were cultured in DMEM with 25 mM glucose (Sigma Aldrich), supplemented with 2 mM L-Glutamine, 15% horse serum (HS), 2.5% FBS, 1% penicillin/streptomycin, in 95% humidified air, with 5% CO₂ at 37°C. Cells were passaged once a week after trypsinization and replaced with new medium twice weekly. Both cell lines were treated with a cytokine cocktail (recombinant murine IL-1 β , specific activity 0.1 U/ml, Peprotech, London, UK, UE; recombinant murine IFN- γ , specific activity 25 U/ml, Peprotech; recombinant murine TNF- α , specific activity 25 U/ml, Peprotech), as previously described (22).

qPCR

Total RNA was extracted with TRIzol (Life Technologies, Foster City, CA, USA), according to the manufacturer's instructions. RNA quantification was performed by Qubit Fluorometer (Life Technologies). Contaminant DNA was removed using deoxyribonuclease 1 (DNase I Amplification Grade; Life Technologies). DNase-treated RNA was reverse transcribed by using a High Capacity RNA-to-cDNA Kit (Life Technologies), according to the manufacturer's instructions. Resulting cDNAs (30 ng per sample) were amplified through an ABI PRISM 7900HT Fast Real-Time PCR System (Life Technologies), as previously described (26). Single-gene specific assays were performed through real-time PCR by using Fast SYBR Green Master Mix (Life Technologies) according to the manufacturer's instruction. To allow statistical analysis, PCRs were performed in three independent biological replicates. The list of the primer pairs used for comparison analysis is reported below.

Gene Symbol	Forward	Reverse
PARP1	CTCTCCAATCGTTCTACAC	GTTGTCTAGCATCTCCACCT
PARP2	CTCCATCCCTCCAGTAATCC	ATTTCAATGTCTCCCAATGCC
PARP3	GAACCTTATCACCACATCTTCAG	GGCATCTTCTCCACATCCAG
PARP4	GATAACAGCACACTTCCCTCC	TTGTCTCTTCAGGTCCTCCAC
TNKS1	GGCATATCCAGAATATCTCATCAC	GGTCACTAGGTCTTCTGCTC
TNKS2	GCCAACCATCCGAAATACAG	CTTATAGTCACCAGTCAGAACAG
PARP6	AGCATCTTCTCACCCATTCC	GAACGATTCATAAGGCGCTCG
PARP7	GAATGAAGTATGGAGGACAAGAC	GAGTTTGAATTACTACAGGGTGG
PARP8	TTCTGGATGAGGAGATTGCTG	ACTGGCCCGTTTAAATACTG
PARP9	GTACACATTCAACGATACCC	CACCTTATTGTCTATCTGCTCC
PARP10	CTTGAAGGAACGGATGTGAC	GACTCTGAAGCAACTCTTGG
PARP11	AAGCAGATGAATCTTGTCC	ACAGATGTAAGTGAAGGCAC
PARP12	CCTGGGATTTAAGAAGTCACTC	AAAGTAGAAAGTGTAGTGTACGG
PARP14	TGCCAAGCAGTCAGTGTGTC	CCTGGAAAACCTGTGTCTCTAT
PARP16	ACCTGAACAAGACTTCTCTG	CCATGAGGACTATAAATGAGGG
Trp53	CACGCTTCTCCGAAGACTGG	TCTTCTGGAGGAAGTAGITCCAT
Mapk8 (JNK1)	TCAAGCACCTTCACTCTGCTG	TCCTCGCCAGTCCAAAATCAA
Mapk9 (JNK2)	TACCAGATGCTCTGTGGCAT	TACAGGCTGTTCGGCGCC
PPIA	CAGAGCCACTGTGCGTTT	TGCTTTGGAACTTTGTCTGCAA
HPRT	CAGTCAACGGGGACATAAA	GGGCTGTACTGCTTAACCAAG

Immunofluorescence

Murine pancreatic α TC1.6 and β TC1 cells were cultured on a sterile circular cover-glass (12 mm diameter, from Electron Microscopy Sciences, PA, USA), inserted in a 24-well plate. After incubation (24 and 48 h), with or without cytokines, cells were processed as previously reported (27). Pancreatic α TC1.6 and β TC1 cells were fixed with 3% paraformaldehyde in phosphate buffered saline (PBS) at 4°C for 30', washed twice with PBS for 5' and permeabilized with 0.2% TritonX-100 in PBS for 10'. Non-specific sites were blocked by incubation in 5% BSA at 20°C for 30'. Subsequently, both cell lines were incubated overnight at 4°C with the primary goat polyclonal antibody against PARP-14 (diluted 1:100 in PBS containing 1% BSA) in a moist chamber. Following three washing steps with PBS for 5', anti-goat FITC-conjugated secondary antibody (Santa Cruz), diluted 1:50 in PBS containing 1% BSA, was added for 1 h at 20°C in a dark chamber. Following the fluorescent labeling procedures, the slides were washed three times (5' each) with PBS, air dried, mounted up-side down on glass slides and covered with a drop of DAPI solution (Electron Microscopy Sciences) to counterstain the nucleus. Negative controls did not include both primary antibodies.

Confocal Microscopy Imaging

For confocal imaging, we used an Olympus FV1000 confocal laser scanning microscope (LSM), equipped with Diode UV (405 nm, 50 mW), multiline Argon (457 nm, 488 nm, 515 nm, total 30 mW), HeNe (543 nm, 1 mW), and HeNe(R) (633 nm, 1 mW) lasers. An oil immersion objective (60x O PLAPO) and spectral filtering system were used. The detector gain was fixed at a constant value; images were acquired at random locations throughout the area in sequential mode. Quantitative

analysis of fluorescence was performed by using the ImageJ software (1.50i version, NIH), in terms of the average of the mean gray value measured at least in 10 equivalent regions of interest (ROIs), drawn in the cell-covered areas. The values obtained by these analysis were imported into the OriginPro 8.6 program for statistical analysis for *p*-values,

TABLE 2 | Expression profile of 15 candidate PARPs in α TC1.6 and β TC1 after treatment with cytokines for 48 h.

PARP family member	Avg $\Delta\Delta$ Ct α TC1.6	Avg $\Delta\Delta$ Ct β TC1	<i>p</i> -value
Parp1	-0.15	0.07	0.66
Parp2	0.01	-0.08	0.87
Parp3	-2.10	-2.68	0.21
Parp4	-0.24	-0.59	0.60
Tnks	0.29	0.02	0.67
Tnks2	0.09	-0.22	0.51
Parp6	-0.06	-0.27	0.57
Parp7	0.23	0.26	0.90
Parp8	-0.08	-0.47	0.51
Parp9	-2.75	-2.49	0.55
Parp10	-2.23	-1.96	0.50
Parp11	-0.37	-1.02	0.10
Parp12	-1.94	-1.62	0.40
Parp14	-8.88	-4.53	0.01
Parp16	-0.53	-0.92	0.38

Expression values are reported as $\Delta\Delta$ Ct, according to a color variation from green to red. Higher $\Delta\Delta$ Cts (in green) correspond to a lower PARP expression instead, lower $\Delta\Delta$ Cts (in red) correspond to a higher PARP expression. PARP14 induction, in bold, is significantly higher in α TC1.6 with respect to β TC1 (*p* = 0.01, *n* = 3, Student's *t*-test).

TABLE 1 | Fold change values of 15 PARP family members in murine pancreatic α TC1.6 and β TC1 cells after 48 h of cytokine treatment.

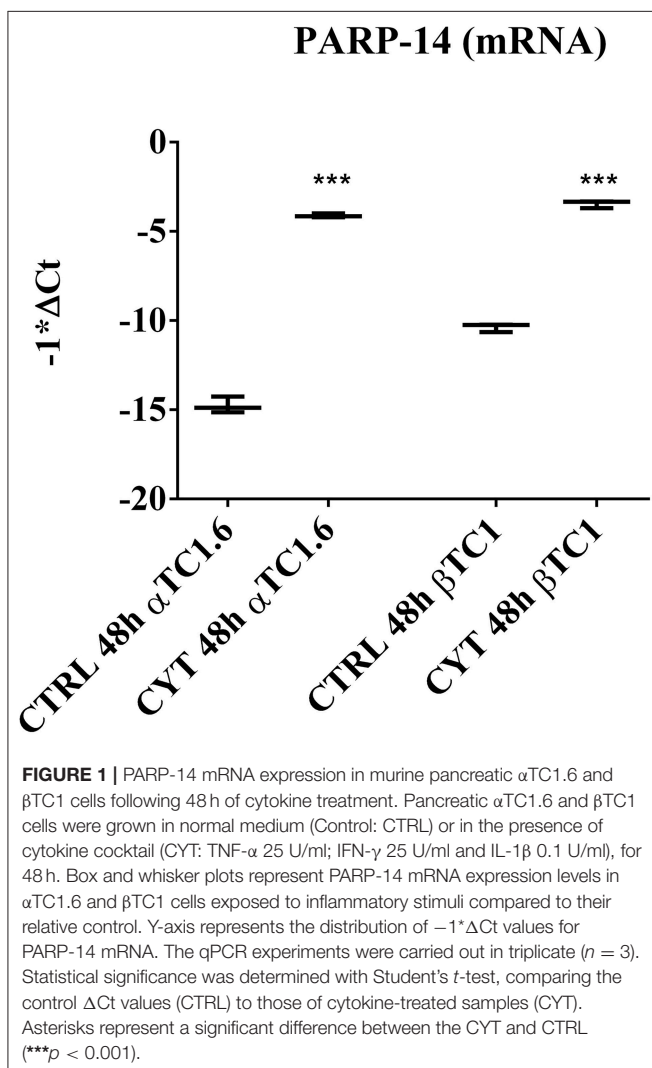
PARP family member	Avg FC α TC1.6 CYT 48 h	Std dev	<i>p</i> -values	Avg FC β TC1 CYT 48 h	Std dev	<i>p</i> -values
Parp1	0.98	±0.39	0.7123734	0.67	±0.21	0.8364281
Parp2	0.98	±0.36	0.9890045	0.82	±0.34	0.8416218
Parp3	5.19	±1.68	0.0265288	6.05	±1.23	0.0046319
Parp4	1.27	±0.74	0.7370967	1.41	±0.07	0.0063723
Tnks	0.82	±0.42	0.6121232	0.81	±0.30	0.9541871
Tnks2	1.02	±0.42	0.8511544	1.23	±0.06	0.0440711
Parp6	1	±0.27	0.8383906	1.11	±0.29	0.3679152
Parp7	1.02	±0.22	0.4051082	0.65	±0.14	0.3227707
Parp8	1.38	±0.62	0.8922677	1.21	±0.21	0.0924684
Parp9	27.88	±1.71	0.0000092	35.48	±0.56	0.0000007
Parp10	3.95	±0.55	0.0035363	3.83	±1.42	0.0305762
Parp11	3.28	±0.16	0.0000512	5.43	±0.68	0.0002361
Parp12	4.27	±0.99	0.0142340	2.61	±0.71	0.0208804
Parp14	2102.5	±13.10	0.0000002	122.48	±0.91	0.0000001
Parp16	1.62	±0.55	0.2686825	1.66	±0.33	0.0345925

Fold change values (Avg FC) of each PARP are reported comparing PARP Δ Ct values of the cells treated with the cytokine (CYT) cocktail (TNF- α 25 U/ml; IFN- γ 25 U/ml and IL-1 β 0.1 U/ml) and PARP Δ Ct values of steady state cells (Control: CTRL), at 48 h. qPCR experiments were carried out in triplicate (*n* = 3). Statistical significance was determined with Student's *t*-test. Std Dev and *p*-value columns indicate the standard deviation values and the significance of every single PARP, respectively.

calculated by using a one-way ANOVA with a Tukey multiple comparison test.

Caspase-3 Colorimetric Protease Assay

Caspase-3 activity was evaluated on α TC1.6 and β TC1 cell lysates through a colorimetric protease assay (Thermo Fisher Scientific), following the manufacturer's protocol. Briefly, cells (α TC1.6 and β TC1) were seeded at a concentration of 5×10^6 cells in 100 mm petri dish for each experimental condition [CTRL; 10 μ M PJ-34; cytokines (CYT: TNF- α 25 U/ml; IFN- γ 25 U/ml and IL-1 β 0.1 U/ml); CYT + 10 μ M PJ-34]. After 24 and 48 h of incubation the cells were lysed and centrifuged at 10,000 g for 1 min at 4°C. The supernatant containing 100 μ g of total protein were incubated with 5 μ L caspase substrate in the 50 μ L reaction buffer at 37°C for 2 h in the dark. The caspase-3 activity was determined by a microplate reader (Synergy 2-bioTek) set at 400 nm.



Imaging Flow Cytometer Analysis

α TC1.6 and β TC1 cells were seeded in 6-well plates at a density of 3×10^4 cells. After incubation for 16 h, the two cell lines were exposed to the treatments. At the appropriate time points, cells were collected, washed with PBS and stained with Annexin V-FITC/Propidium Iodide (PI), in Annexin-V binding buffer (Sigma-Aldrich), according to the manufacturer's instructions. Cells were incubated for 10' at 20°C and protected from light. Samples were analyzed immediately by flow cytometer FlowSight[®] (Amnis[®], part of EMD Millipore) as previously reported (28). A 488 nm laser was used for excitation. Bright field (430–480 nm), Annexin V-FITC (505–560 nm) and PI (595–642 nm) analysis were focused on at least 5,000 cell events per sample. INSPIRE[®] software (<http://www.merckmillipore.com>) was used to setup, calibrate and obtain spectral compensation, while IDEAS[®] [version 6.0 software (<http://www.merckmillipore.com>)] was used to quantify the numbers of vital (Annexin V and PI negative, double negative), early apoptotic (Annexin V positive/PI negative), late apoptotic (Annexin V and PI positive, double positive) and necrotic cells (PI positive). The distribution of acquired events in the scatter plot, depending on their differential fluorophore labeling, is shown in the results section.

Western Blot

The expression of PARP-14, JNK1 and JNK2, and the level of phospho-p53 were evaluated by western analysis. Pancreatic α TC1.6 and β TC1 cells were grown for 24 and 48 h with normal medium (control) or stimulated by a cytokine cocktail, either in the presence or in the absence of 10 μ M PJ-34 inhibitor (added simultaneously). Cells were lysed as previously described (29, 30). Cell lysate proteins were quantified with a bicinchoninic acid (BCA) protein assay kit (Pierce[™], ThermoFisher Scientific). Immunoblots (30 μ g cell lysate proteins) were performed as described elsewhere (29). Membranes were incubated with primary antibodies against PARP-14 (mouse monoclonal antibody, 1:500 dilution), JNK1 (rabbit polyclonal antibody, 1:5000 dilution), JNK2 (rabbit polyclonal, 1:4000), phospho-p53 (rabbit polyclonal antibody, 1:1000 dilution) and total p53 (mouse monoclonal antibody 1:1000). Membranes were then incubated with secondary antibodies for 1 h at 20°C and immune complexes were detected by an enhanced chemiluminescence reagent (ECL, Amersham). Relative phosphorylation or protein levels were quantified by using the ImageJ program. Immunoblots were normalized through GAPDH mouse monoclonal antibody (1:2000 dilution).

Statistical Analysis

Data are expressed as mean \pm standard deviation (S.D.) of three independent experiments (i.e., biological and technical triplicates). We evaluated the statistical significance of these data by applying Student's t -test or one-way Anova test, as described in figure legends.

RESULTS

PARP Family Expression in Pancreatic α TC1.6 and β TC1 Cells Treated With Inflammatory Cytokines for 24 and 48 h

By qPCR, we verified if any member of the PARP family was differentially expressed (DE) in pancreatic α TC1.6 and β TC1 cell lines, in the presence of the following cytokine concentrations: TNF- α 25 U/ml; IFN- γ 25 U/ml and IL-1 β

0.1 U/ml, compared with the steady state, at 24 h (Table S1) and 48 h (Table 1). These cytokine concentrations were chosen after dose-response and time-course experiments, evaluated by MTT and FACS analysis (data not shown). In the presence of an inflammatory environment, significant fold change values were found for many PARPs, in α TC1.6 and β TC1, at both 24 h (Table S1) and 48 h (Table 1). Notwithstanding, PARP-14 was the only one of the PARP family that was significantly differentially expressed between the two cell lines (Table 2). The

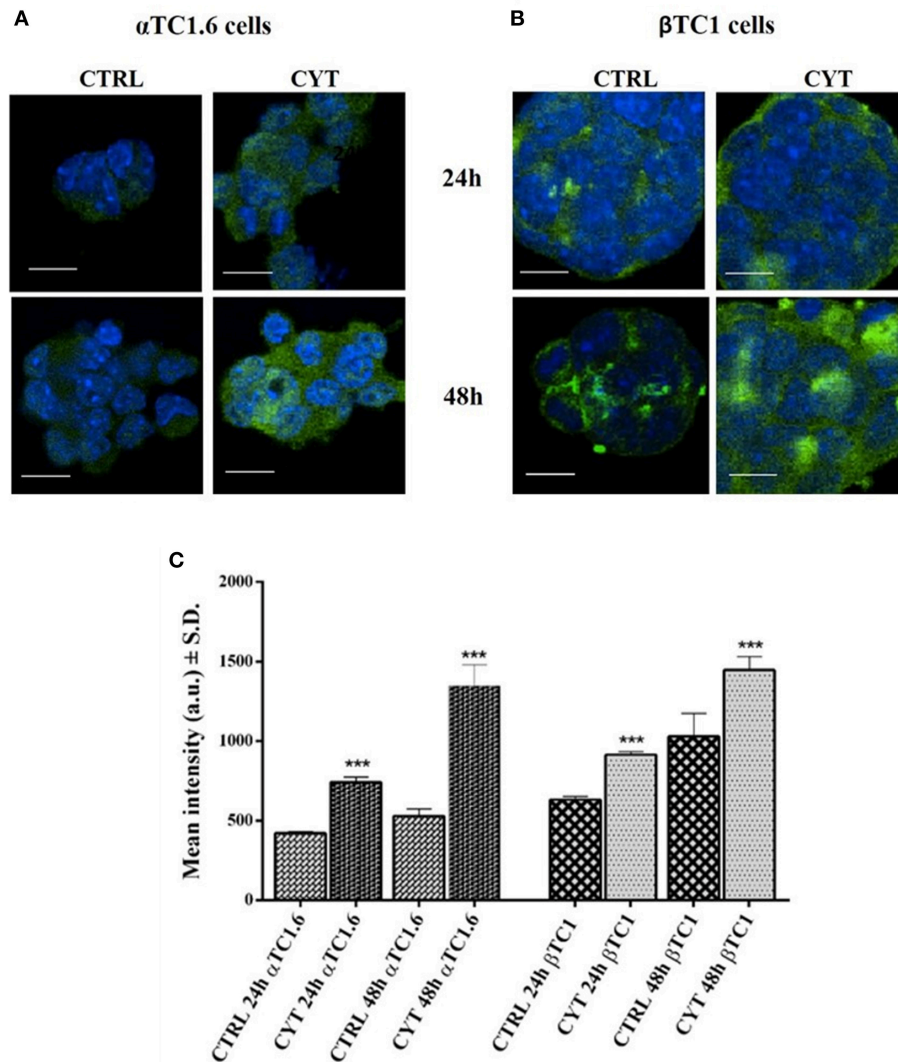


FIGURE 2 | Confocal LSM of PARP-14 expression in pancreatic α TC1.6 and β TC1 cells, following 24 and 48 h of cytokine treatment. Confocal microscopy of PARP-14 expression in pancreatic α TC1.6 (A) and β TC1 cells (B). The two cell lines were cultured in normal medium (Control: CTRL) or in medium containing cytokines (CYT: TNF- α 25 U/ml; IFN- γ 25 U/ml, and IL-1 β 0.1 U/ml) for 48 h. Cells were stained with a polyclonal anti-goat FITC-conjugated secondary antibody. Green fluorescence represents the distribution of PARP-14 inside the cells. The blue fluorescence is due to the labeling with DAPI to mark the nuclei. The images were recorded at the following conditions of excitation/emission wavelengths: 405/425–475 nm (blue); 488/500–540 nm (green). Magnification x60; Scale bar = 20 μ m. Quantitative analysis of Confocal LSM data (C). The graphs show mean intensity values (a.u.) of PARP-14 fluorescence as measured on the confocal LSM \pm S.D. (= standard deviation). Student's *t*-test was performed by using the data from 4 to 6 randomly chosen fields and a minimum of 10 cells in each field of the control sample (CTRL) compared to those of cytokines (CYT). All experiments were repeated 3 times ($n = 3$). Asterisks represent a significant difference between the CYT and CTRL (** $p < 0.001$).

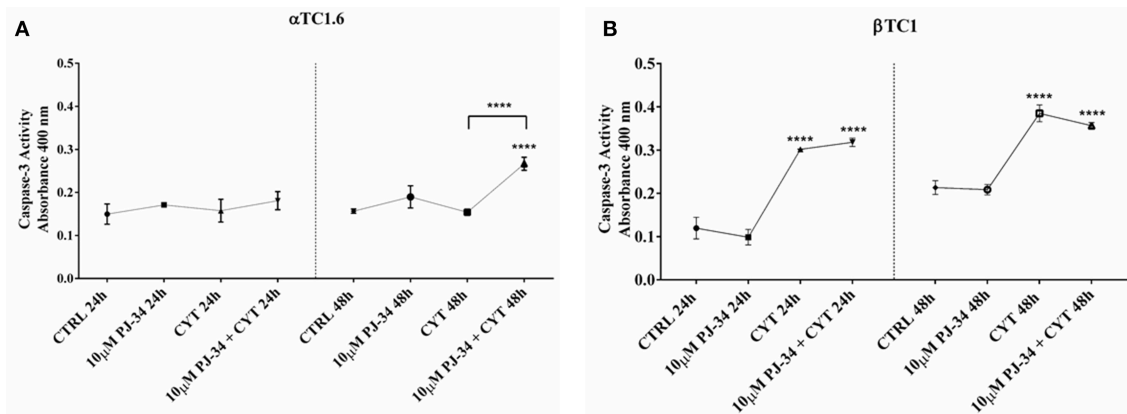


FIGURE 3 | Caspase-3 activity of α TC1.6 and β TC1 cells following 24 and 48 h of cytokine treatment, in the presence or absence of 10 μ M PJ-34. Pancreatic α TC1.6 (A) and β TC1 cells (B) were cultured in full medium with (CYT) or without (Control: CTRL) cytokine cocktail (TNF- α 25 U/ml; IFN- γ 25 U/ml, IL-1 β 0.1 U/ml), both in the presence or absence of 10 μ M PJ-34, for 24 and 48 h. Caspase-3 activity was evaluated through a colorimetric protease assay, as described in the Materials and Methods section. In Y-axis are reported the means \pm SD of absorbance values of each experimental condition (X-axis) at 24 and 48 h (S.D. = standard deviation). All experiments were repeated 3 times ($n = 3$). Statistical analysis was performed by One-way Anova test, using control (CTRL) and cytokines (CYT) conditions as reference sample. Asterisks represent a significant difference between the treated samples and CTRL. The significance between CYT + 10 μ M PJ-34 and CYT is indicated by the asterisks upon the sticks (**** $p < 0.0001$).

high expression levels of PARP-14 in α TC1.6 cells, compared with those obtained in β TC1 cells, allowed us to hypothesize a potentially important role of PARP-14 in α TC1.6 cells. As a valid reference model to study cell survival in an inflammatory state, we selected β TC1 cells, since they are very susceptible to the action of cytokines.

mRNA Expression of PARP-14 in Pancreatic α TC1.6 and β TC1 Cells, Following 24 and 48 h of Cytokine Treatment

The box plots in **Figure 1** show the different expression levels of PARP-14 mRNA between the two pancreatic cell phenotypes, after treatment with cytokines at 48 h (**Figure 1**). According to the data shown in **Tables 1, 2**, the inflammatory state induced a significant increase of PARP-14 mRNA expression levels in both cell lines, though this increment was significantly higher in α TC1.6 cells. A similar trend was observed in the same experimental conditions at 24 h (**Figure S1**).

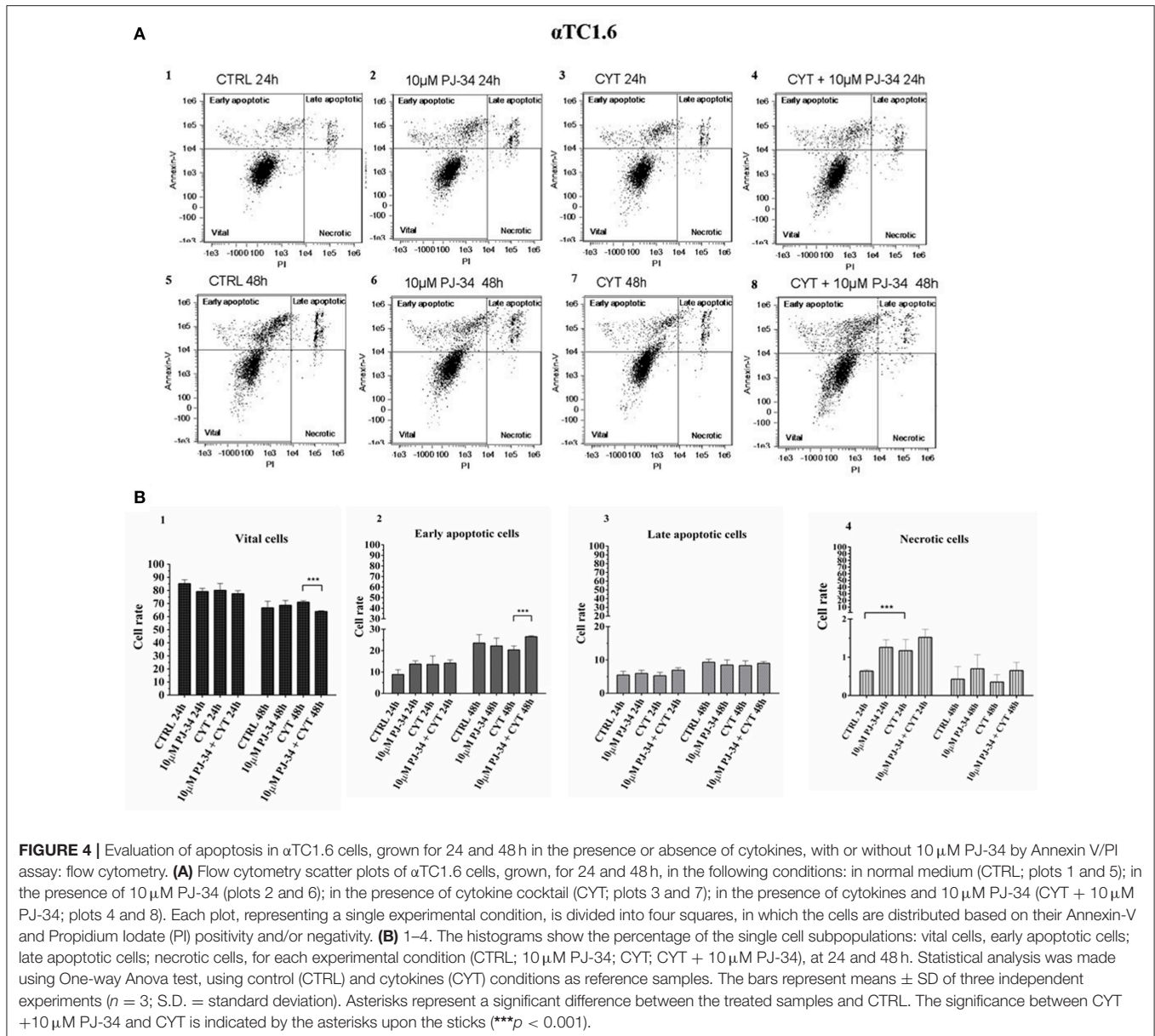
PARP-14 Protein Expression in Pancreatic α TC1.6 and β TC1, Following 24 and 48 h of Cytokine Treatment: Confocal Microscopy Analysis

The expression of PARP-14 in murine pancreatic α TC1.6 and β TC1 cells treated with or without cytokines (TNF- α 25 U/ml; IFN- γ 25 U/ml and IL-1 β 0.1 U/ml) for 24 and 48 h, was analyzed through laser scanning confocal microscopy analysis (**Figure 2**). By using a green fluorescently-labeled antibody (FITC secondary antibody), we analyzed PARP-14 immunofluorescence in α TC1.6 and β TC1 cells, grown for 24 and 48 h in normal culture medium

(controls) or in the presence of inflammatory cytokines, at the concentrations mentioned above (**Figures 2A,B**). In α TC1.6 cells, the treatment with cytokines induced a significant increase of the PARP-14 immunofluorescence signal, compared with the control, mainly at 48 h (**Figure 2A**). However, in β TC1 cells the PARP-14 immunofluorescence signal was higher in the presence of cytokines and the basal level appears more evident than α TC1.6, especially at 48 h (**Figure 2B**). Therefore, despite the increment of PARP-14 immunofluorescence in both cell lines, this protein was more overexpressed in α TC1.6 than β TC1 cells, particularly at 48 h (**Figures 2A,B**). Quantitative analysis of confocal micrographs was carried out to analyze the fluorescence recorded for the FITC secondary antibodies (**Figure 2C**). In both cell types, there was a statistically significant increase of the fluorescence intensity for PARP-14 after cytokine treatment, however, at 48 h, in α TC1.6 cells, the intensity almost doubled that measured at 24 h, compared to that measured for β TC1 cells.

Caspase-3 Activity in Pancreatic α TC1.6 and β TC1 Cells, Following 24 and 48 h of Cytokine Treatment, in the Presence or Absence of PJ-34

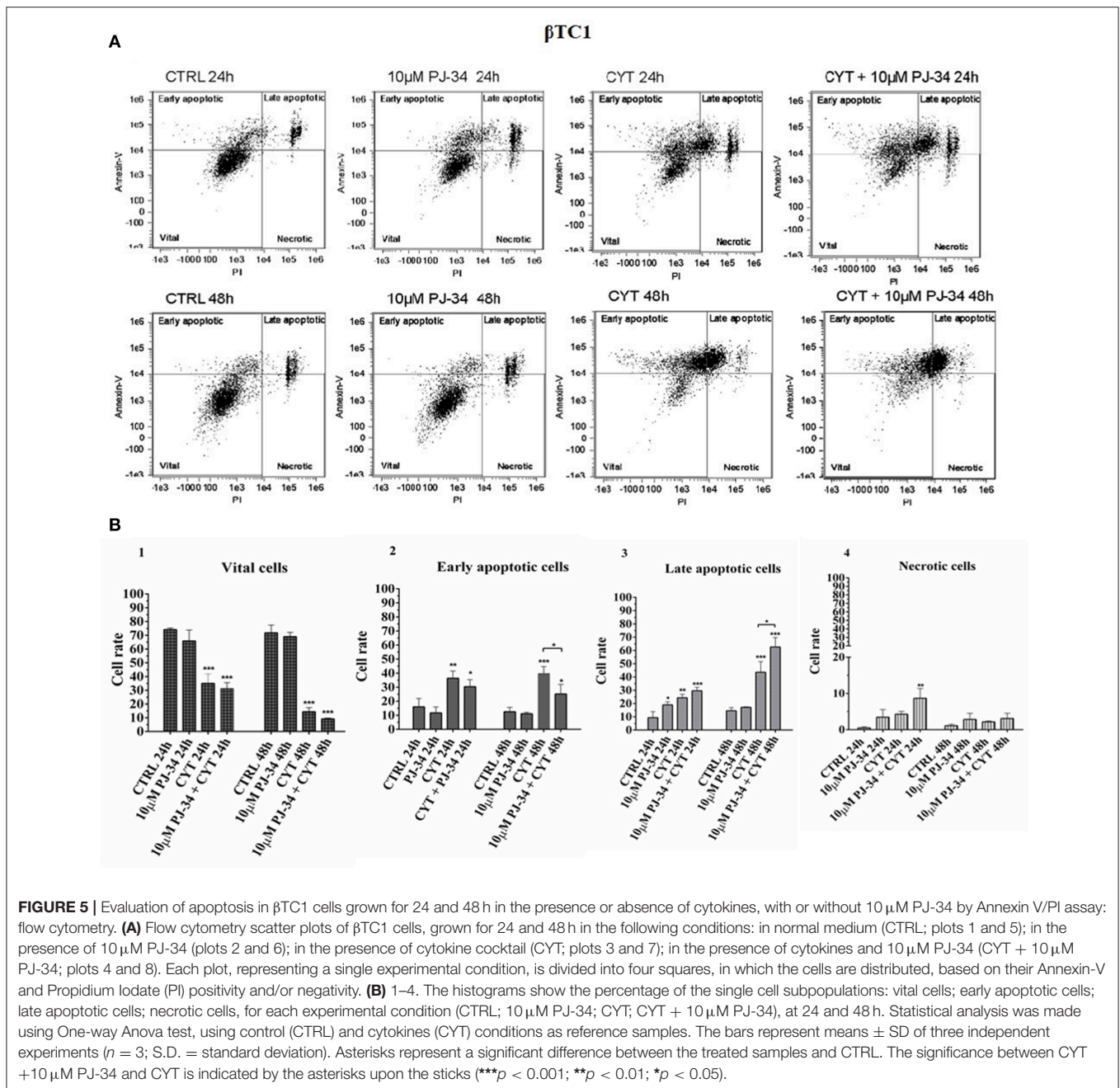
Caspase-3 assay was performed on pancreatic α TC1.6 and β TC1 cell lines to evaluate apoptosis induction by the cytokine cocktail. Furthermore, we also tested the effects of the PARP inhibitor PJ-34 on the biomolecular functions of PARP-14. The graphs in **Figure 3** show the caspase-3 activity of α TC1.6 (**Figure 3A**) and β TC1 (**Figure 3B**), treated with cytokines (TNF- α 25 U/ml; IFN- γ 25 U/ml and IL-1 β 0.1 U/ml), in the presence or absence of 10 μ M PJ-34, at 24 and 48 h. Unlike β TC1 cells, cytokine treatment of α TC1.6 did not cause



significant changes in the caspase-3 activity, at both 24 and 48 h (Figures 3A,B). No variation of the caspase-3 activity was observed when 10 μ M PJ-34 was added, simultaneously, to the cytokines, at 24 h, in both cell lines (Figures 3A,B). However, at 48 h, the addition of PJ-34 to the cytokines produced a different result in the two cell lines. In fact, while in β TC1 cells the addition of the PARP inhibitor did not produce any significant effects on the caspase-3 activity, in α TC1.6 cells the presence of PJ-34 caused a significant increase of the enzymatic activity compared to the cytokines alone (Figure 3A). This result could suggest a protective role of PARP-14 in α TC1.6.

Evaluation of Apoptotic Death on Pancreatic α TC1.6 and β TC1 Cells Grown With Cytokines, in the Presence or Absence of 10 μ M PJ-34: Flow Cytometry Assay

To verify the potential protective function of PARP-14 in this system, flow cytometry analysis was carried out on α TC1.6 and β TC1 cells, grown in the presence or the absence of 10 μ M PJ-34. This technique analyzes the percentage of vital, early/late apoptotic and necrotic cells, for each experimental condition [i.e., control, 10 μ M PJ-34, cytokines (TNF- α 25



U/ml; IFN- γ 25 U/ml and IL-1 β 0.1 U/ml) and cytokines + 10 μ M PJ-34]. Representative data of the Annexin V-FITC/Propidium Iodide (PI) flow cytometry experiments are shown in **Figures 4A,B, 5A,B**.

Effect of PJ-34 on Apoptotic α TC1.6 Cell Death, Following 24 and 48 h of Cytokine Treatment

Each scatter plot shown in **Figure 4A** represents the distribution, in four squares, of pancreatic α TC1.6 cells according to their

staining with Annexin-V and PI. At both 24 and 48 h the distribution of α TC1.6 cells was similar in all experimental conditions, indicating the resistance of these cells to apoptosis induction by inflammatory cytokines (**Figure 4A, 1–8**). The histograms shown in **Figure 4B, 1–4**, show the percentage of each cell subpopulation (vital, early/late apoptotic, necrotic) in the experimental conditions. It was interesting to note that cytokine treatment did not significantly affect α TC1.6 cell survival (**Figure 4B, 1–4**). However, only at 24 h, in the presence of cytokines, was a significant increment of necrotic cell rate, compared with the control, observed. However, the

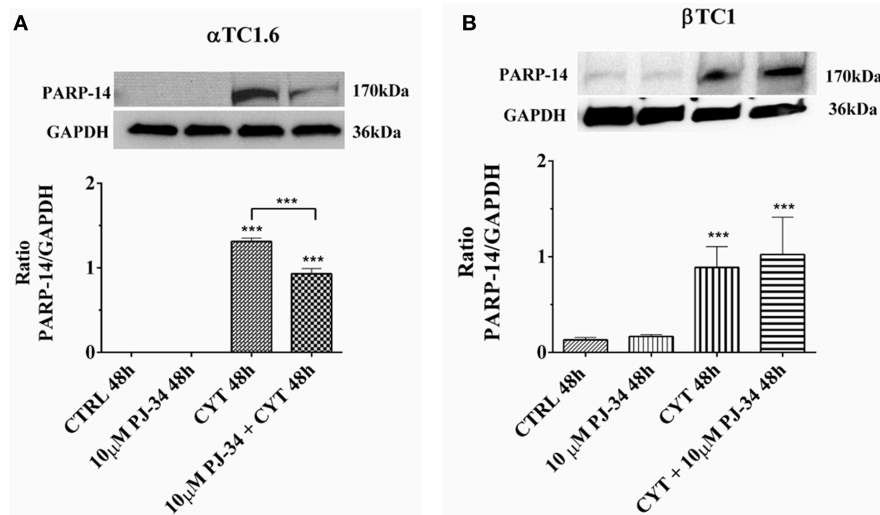


FIGURE 6 | Effect of the PARP inhibitor PJ-34 on PARP-14 expression in α TC1.6 and β TC1 cells, grown for 48 h in the presence or absence of cytokines. α TC1.6 (A) and β TC1 (B) cells were grown in normal culture medium: control (CTRL); in the presence of 10 μ M PJ-34; in culture medium containing cytokine cocktail (CYT: TNF- α 25 U/ml; IFN- γ 25 U/ml, and IL-1 β 0.1 U/ml); in culture medium with the addition of both cytokine cocktail and 10 μ M PJ-34 (CYT + 10 μ M PJ-34), for 48 h. Expressed protein was revealed with a mouse monoclonal antibody against PARP-14 (1:500 dilution) as described in Materials and Methods section. The blots were controlled for equal loading by GAPDH, using a mouse monoclonal antibody (1:2000 dilution). Immunoreactive bands were visualized by chemiluminescence (ECL system). The values were obtained by the reading of blots using the Image J program. Statistical analysis was made using One-way Anova test, using control (CTRL) and cytokines (CYT) conditions as reference samples. The bars represent means \pm SD of three independent experiments (S.D. = standard deviation). Asterisks represent a significant difference between the treated samples and CTRL. The significance between CYT + 10 μ M PJ-34 and CYT is indicated by the asterisks upon the sticks (***) $p < 0.001$.

percentage of the necrotic cell subpopulation was under 2% of the total cells, in all the experimental conditions and at both time points. Furthermore, the concomitant presence of both PJ-34 and cytokines for 48 h caused a significant reduction of vital cells and a significant increase of the number of early apoptotic cells. This result convincingly suggests that the inhibition of PARP-14 makes pancreatic α TC1.6 cells susceptible to an inflammatory environment.

Effect of PJ-34 on Apoptotic β TC1 Cell Death, Following 24 and 48 h of Cytokine Treatment

The distribution of the β TC1 cell population shown in the scatter plots, under inflammatory stimuli, appears very different with respect to α TC1.6 (Figure 5A, 1–8). In fact, when β TC1 were grown in the presence of cytokines alone or in combination with PJ-34, most of these cells were scattered within the upper quadrants, proving that they were undergoing apoptosis, mainly at 48 h. The histograms in Figure 5B, 1–4 show the percentage of β TC1 cell subpopulations (vital, early/late apoptotic and necrotic cells) shown in the scatter plots (Figure 5A, 1–8). It is evident that the inflammatory cytokines caused a sudden and drastic reduction of vital cells and a concomitant increase of early/late apoptotic and necrotic cells, independently of the addition of the PARP inhibitor, at both time points. This confirms the susceptibility of beta cells to inflammation.

Evaluation of PAR-14, JNK1, and JNK2 Expression and p53 Phosphorylation in Pancreatic α TC1.6 and β TC1 Cells Grown, for 24 and 48 h, With Cytokines, in the Presence or Absence of 10 μ M PJ-34: Western Blot Analysis

To examine the potential signaling involvement of PARP-14 in a survival transduction pathway, mediated by c Jun N-terminal kinases 1 and 2 (JNK1/2), we performed a series of qPCR and western analysis on α TC1.6 and β TC1 cells, grown in the presence or the absence of cytokines, with or without PJ-34, for 24 and 48 h. Furthermore, we also studied the activation of one of the most common apoptosis mediators, the phosphorylated p53 protein.

Effect of the PARP Inhibitor PJ-34 on PARP-14 Expression in α TC1.6 and β TC1 Cells, Grown for 24 and 48 h in the Presence or Absence of Cytokines

As a first approach, we verified how the inhibitor PJ-34 modulates the expression of PARP-14 both in α TC1.6 and β TC1 cells in our experimental conditions (Figures 6A,B and Figures S2A,B). The expression of PARP-14 in α TC1.6 cells was not detectable at the basal level (control and PJ-34 alone), at 24 h (Figure S2A) as well as 48 h (Figure 6A). On the other

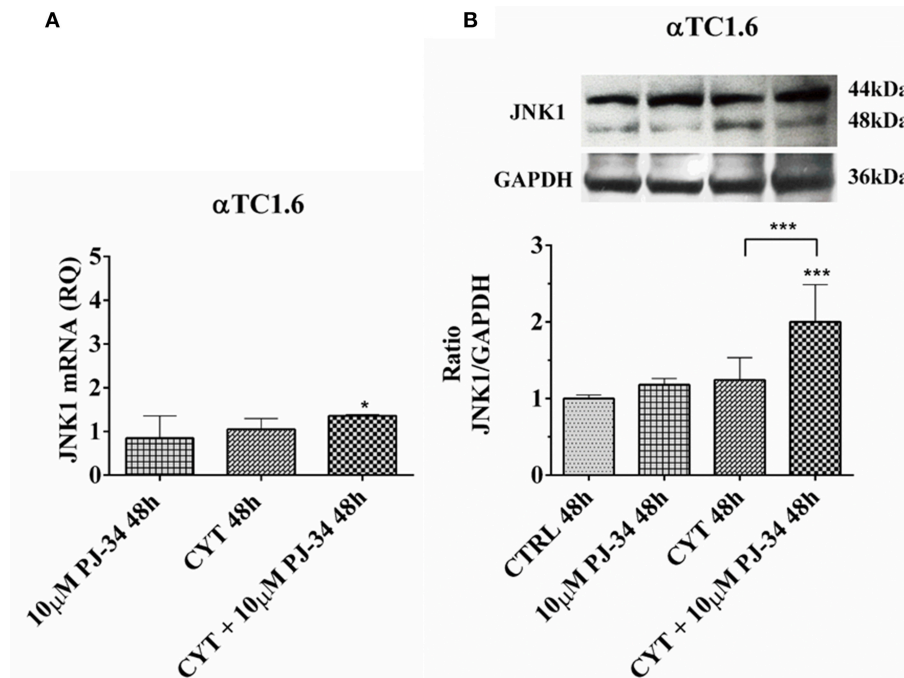


FIGURE 7 | Effect of the PARP inhibitor PJ-34 on JNK1 mRNA and protein expression in α TC1.6 cells, grown for 48 h in the presence or absence of cytokines. Real-time PCR and total cell lysate immunoblottings were performed as described in the Materials and Methods section. α TC1.6 cells were grown: in normal culture medium (control: CTRL); in the presence of 10 μ M PJ-34; in culture medium containing cytokine cocktail (CYT: TNF- α 25 U/ml; IFN- γ 25 U/ml and IL-1 β 0.1 U/ml); in culture medium with the addition of both cytokine cocktail and 10 μ M PJ-34 (CYT + 10 μ M PJ-34), for 48 h. **(A)** Relative quantity (RQ) level of JNK1 mRNA, at 48 h, in the experimental conditions mentioned above. Relative quantification is referred to untreated cells. **(B)** JNK1 protein was revealed with a rabbit polyclonal antibody (1:5000 dilution) as described in Materials and Methods section. The blots were controlled for equal loading by GAPDH, using a mouse monoclonal antibody (1:2000 dilution). Immunoreactive bands were visualized by chemiluminescence (ECL system). The values were obtained by the reading of blots through the Image J program. Statistical analysis was carried out by One-way Anova test, using control (CTRL) and cytokines (CYT) conditions as reference samples. The bars represent means \pm SD of three independent experiments (S.D. = standard deviation). Asterisks represent a significant difference between the treated samples and CTRL. The significance between CYT + 10 μ M PJ-34 and CYT is indicated by the asterisks upon the sticks (*** p < 0.001; * p < 0.05).

hand, cytokine exposition caused a significant increase of PARP-14 expression, mainly at 48 h (Figure 6A). At the same time point, the addition of PJ-34 to the cytokines significantly reduced PARP-14 expression (Figure 6A). In β TC1 cells, the increase of the protein level observed in an inflammatory environment was not reversed by the addition of PJ-34, both at 24 h (Figure S2B) and 48 h (Figure 6B).

Effect of the PARP Inhibitor PJ-34 on JNK1 mRNA and Protein Expression in α TC1.6 Cells, Grown for 24 and 48 h in the Presence or Absence of Cytokines

Since JNK1 is a pro-apoptotic molecule, activated by inflammatory signals, we wondered what the behavior of this protein in our experimental model could be. The trend of JNK1 mRNA was close to that of its encoded protein at both 24 h (Figures S3A,B) and 48 h (Figures 7A,B). After 24 h of treatment with cytokines, there was no significant reduction of the JNK1 mRNA levels, instead the JNK1 protein expression levels appeared significantly reduced vs. control (Figures S3A,B). This indicates the resistance of these cells to inflammatory insults. At the same time point, the addition of 10 μ M PJ-34 to the

cytokines did not produce any significant effect on both mRNA and protein levels (Figures S3A,B). Conversely, at 48 h, the addition of the inhibitor PJ-34 to the cytokines up-regulated JNK1 mRNA compared with the control and protein expression compared with the control and cytokines alone (Figures 7A,B).

Effect of the PARP Inhibitor PJ-34 on JNK1 mRNA and Protein Expression in β TC1 Cells, Grown for 24 and 48 h in the Presence or Absence of Cytokines

In β TC1 cells, no differences in JNK1 mRNA expression levels were observed at 24 h (Figure S4A). However, at the same time point, cytokines was able to induce a significant increase of JNK1 protein (Figure S4B). Cytokines and PJ-34, in combination, down-regulated JNK1 protein levels (Figure S4B). At 48 h, it is possible to observe a significant increment of JNK1 protein in the presence of cytokines alone and a significant increase of both mRNA and protein levels in the presence of the combination of cytokines with 10 μ M PJ-34, compared with control (Figures 8A,B).

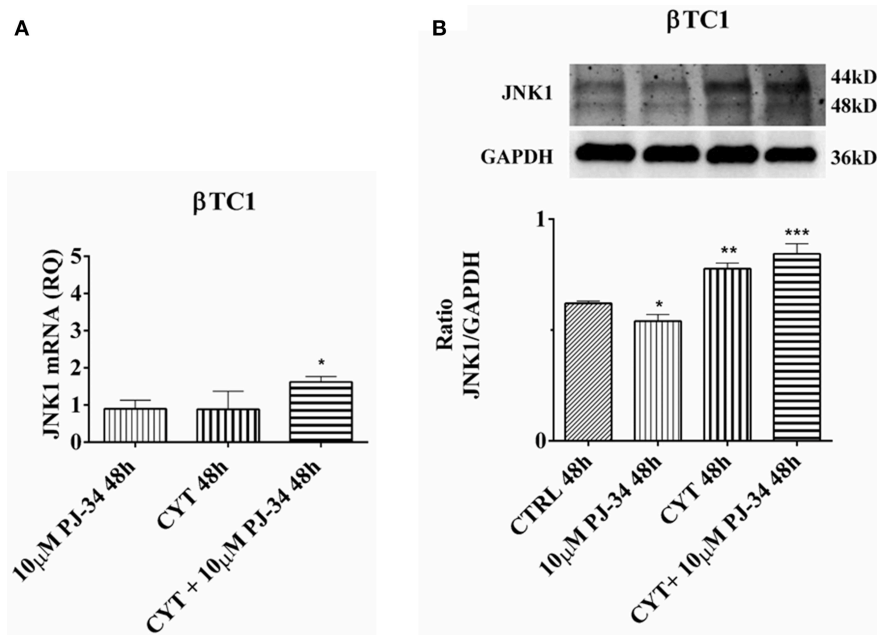


FIGURE 8 | Effect of the PARP inhibitor PJ-34 on JNK1 mRNA and protein expression in β TC1 cells, grown for 48 h in the presence or absence of cytokines. Real-time PCR and total cell lysate immunoblottings were performed as described in the Materials and Methods section. β TC1 cells were grown: in normal culture medium (control: CTRL); in the presence of 10 μ M PJ-34; in culture medium containing cytokine cocktail (CYT: TNF- α 25 U/ml; IFN- γ 25 U/ml; IL-1 β 0.1 U/ml); in culture medium with the addition of both cytokine cocktail and 10 μ M PJ-34 (CYT + 10 μ M PJ-34), for 48 h. **A.** Relative quantity (RQ) level of JNK1 mRNA, at 48 h, in the experimental conditions mentioned above. Relative quantification is referred to untreated cells. **(B)** JNK1 protein was revealed with a rabbit polyclonal antibody (1:5000 dilution) as described in Materials and Methods section. The blots were controlled for equal loading by GAPDH, using a mouse monoclonal antibody (1:2000 dilution). Immunoreactive bands were visualized by chemiluminescence (ECL system). The values were obtained by the reading of blots through the Image J program. Statistical analysis was carried out by One-way Anova test, using control (CTRL) and cytokines (CYT) conditions as reference samples. The bars represent means \pm SD of three independent experiments (S.D. = standard deviation). Asterisks represent a significant difference between the treated samples and CTRL (*** p < 0.001; ** p < 0.01; * p < 0.05).

Effect of the PARP Inhibitor PJ-34 on JNK2 mRNA and Protein Expression in α TC1.6 Cells, Grown for 24 and 48 h in the Presence or Absence of Cytokines

No notable effect was found on JNK2 mRNA expression levels in all experimental conditions, at both 24 h (Figure S5A) and 48 h (Figure 9A). Conversely, JNK2 protein expression levels were significantly reduced when α TC1.6 were grown in the presence of both cytokines and PJ-34, compared with control and cytokines alone, for 24 h (Figure S5B). At 48 h, a significant increase of JNK2 expression was detected in the presence of cytokines compared with the control and in presence of the combination of cytokines with 10 μ M PJ-34 compared with both control and cytokines alone (Figure 9B).

Effect of the PARP Inhibitor PJ-34 on JNK2 mRNA and Protein Expression in β TC1 Cells, Grown for 24 and 48 h in the Presence or Absence of Cytokines

In β TC1 cells, JNK2 mRNA and protein expression levels did not show any significant variation in our experimental conditions, at both 24 h (Figures S6A,B) and 48 h (Figures 10A,B).

Effect of the PARP Inhibitor PJ-34 on p53 mRNA and p53 Phosphorylated Protein Levels in α TC1.6, Grown for 24 and 48 h in the Presence or Absence of Cytokines

To verify the activation of the apoptotic cascade, in our experimental conditions, we analyzed the mRNA expression and the phosphorylation levels of p53 in both cell lines.

In α -cells, no significant variation of both p53 mRNA and protein levels were noted at 24 h, in the conditions tested (Figures S7A,B). At 48 h, cytokine treatment caused a significant increment of the p53 phosphorylated form vs. control (Figure 11B). At the same time point, the presence of both cytokines and PJ-34 induced a significant increase of mRNA compared with the control and the phosphorylated protein against control and cytokines alone (Figures 11A,B).

Effect of the PARP Inhibitor PJ-34 on p53 mRNA and p53 Phosphorylated Protein Levels in β TC1 Cells, Grown for 24 and 48 h in the Presence or Absence of Cytokines

In β TC1 cells, at 24 h, no significant variation was detected in p53 mRNA expression and in its phosphorylation level (Figures S8A,B). At 48, the inflammatory state did not induce

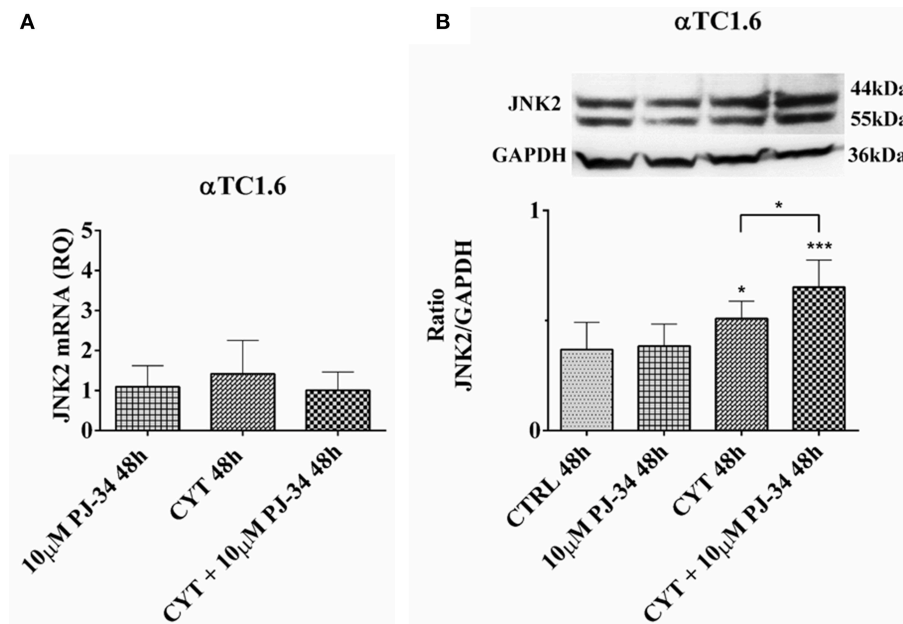


FIGURE 9 | Effect of the PARP inhibitor PJ-34 on JNK2 mRNA and protein expression in α TC1.6 cells, grown for 48 h in the presence or absence of cytokines. Real-time PCR and total cell lysate immunoblottings were performed as described in the Materials and Methods section. α TC1.6 cells were grown: in normal culture medium (control: CTRL); in the presence of 10 μ M PJ-34; in culture medium containing cytokine cocktail (CYT: TNF- α 25 U/ml; IFN- γ 25 U/ml and IL-1 β 0.1 U/ml); in culture medium with the addition of both cytokine cocktail and 10 μ M PJ-34 (CYT + 10 μ M PJ-34), for 48 h. **(A)** Relative quantity (RQ) level of JNK2 mRNA, at 48 h, in the experimental conditions mentioned above. Relative quantification is referred to untreated cells. **(B)** JNK2 protein was revealed with a rabbit polyclonal antibody (1:4000 dilution) as described in Materials and Methods section. The blots were controlled for equal loading by GAPDH, using a mouse monoclonal antibody (1:2000 dilution). Immunoreactive bands were visualized by chemiluminescence (ECL system). The values were obtained by the reading of blots through the Image J program. Statistical analysis was carried out by One-way Anova test, using control (CTRL) and cytokines (CYT) conditions as reference samples. The bars represent means \pm SD of three independent experiments (S.D. = standard deviation). Asterisks represent a significant difference between the treated samples and CTRL. The significance between CYT + 10 μ M PJ-34 and CYT is indicated by the asterisks upon the sticks (** p < 0.001; * p < 0.05).

a significant variation in mRNA expression (Figure 12A). However, it is evident that the p53 phosphorylation level in the presence of cytokines and cytokines + 10 μ M PJ-34 doubled the value of control (Figure 12B). This could indicate that, at this time point, cytokine stimulation is able to trigger the apoptotic death of β TC1 cells, mediated by the p53 protein, independently of the presence of PJ-34.

DISCUSSION

PARP family members are involved in a large variety of physiological and pathological events (5, 31, 32). Until now, most studies have focused on PARP-1, initially as an enzyme involved only in DNA repair, but subsequently also in apoptotic and necrotic cell death and in cancer (4, 33, 34). Nevertheless, what is biologically interesting about these proteins is that they can play a key role also in cell proliferation and survival (35). In fact, in a previous paper, we published data on the involvement of PARP-1 in a DNA independent way within the Extracellular-Regulated-Kinase (ERK) signaling cascade, which regulates cell proliferation and migration of rat brain microvascular endothelial cells. Furthermore, we showed the ability of the PARP inhibitor PJ-34 to regulate PARP-1 mRNA and protein expression. Indeed, by binding the catalytic site of the enzyme, PJ-34 was able

to affect both the enzymatic functions and PARP binding to target proteins (1, 36). Many published studies report that PARP inhibitors promote cancer cell death, as they block the process of repairing damaged DNA (27, 34, 37–41). However, these studies mainly concern PARP-1 (1–3, 42, 43). Despite this, other members of the PARP superfamily could also play a decisive role in regulating various cellular processes including inflammation and immunity (44). In this study, the authors demonstrated that PARP-14 represents an important co-factor of signal transduction and activation of transcription 6 (STAT-6), which is involved in B cell and T cell responses to interleukin-4 (IL-4), mainly in the differentiation of T helper type 2 (Th2) cells. Furthermore, in PARP-14 deficiency mice or those subjected to pharmacological block of PARP-14 activity, the development of T follicular helper (Tfh) cells and the differentiation of Th17 cells are compromised in both *in vitro* and *in vivo* models (44). A further study reports that PARP-14 is involved in the survival pathway in multiple myeloma (MM) (16). Very interesting data in this paper showed that PARP-14 overexpression totally prevented myeloma cells from undergoing apoptosis, induced by JNK2 knockdown: this suggests that PARP-14 is essential in JNK2 dependent survival signaling. PARP-14 is able to bind and inhibit JNK1 that promotes apoptosis by phosphorylating several downstream transcription factors (21, 45). In our study,

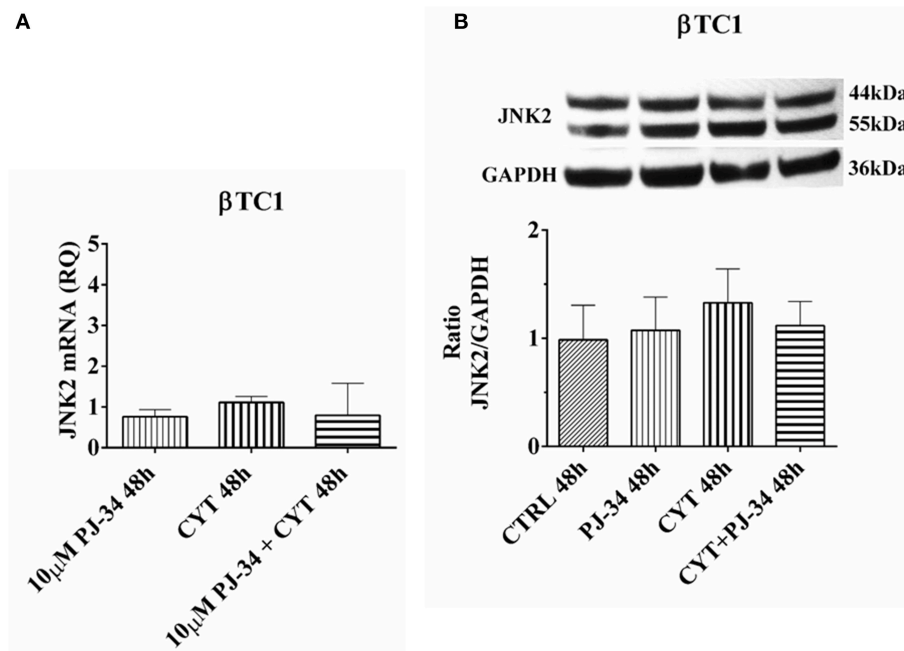


FIGURE 10 | Effect of the PARP inhibitor PJ-34 on JNK-2 mRNA and protein expression in β TC1 cells, grown for 48 h in the presence or absence of cytokines. Real-time PCR and total cell lysate immunoblottings were performed as described in the Materials and Methods section. β TC1 cells were grown: in normal culture medium (control: CTRL); in the presence of 10 μ M PJ-34; in culture medium containing cytokine cocktail (CYT: TNF- α 25 U/ml; IFN- γ 25 U/ml and IL-1 β 0.1 U/ml); in culture medium with the addition of both cytokine cocktail and 10 μ M PJ-34 (CYT + 10 μ M PJ-34), for 48 h. **(A)** Relative quantity (RQ) level of JNK2 mRNA, at 48 h, in the experimental conditions mentioned above. Relative quantification is referred to untreated cells. **(B)** JNK2 protein was revealed with a rabbit polyclonal antibody (1:4000 dilution) as described in Materials and Methods section. The blots were controlled for equal loading by GAPDH, using a mouse monoclonal antibody (1:2000 dilution). Immunoreactive bands were visualized by chemiluminescence (ECL system). The values were obtained by the reading of blots through the Image J program. Statistical analysis was carried out by One-way Anova test, using control (CTRL) and cytokines (CYT) conditions as reference samples. The bars represent means \pm SD of three independent experiments (S.D. = standard deviation).

the expression analysis of murine PARP family members by qPCR allowed us to highlight an over-expression of many PARPs in both cell lines, under inflammatory state. Nevertheless, we focused on PARP-14 because: (1) its induction was significantly higher in α TC1.6 than in β TC1, after treatment with cytokines, (see Table 2); (2) recent literature data report its involvement in a survival pathway that can justify a critical role played by PARP-14 in α cell survival (16, 17). Through expression studies, carried out by qPCR, western blot and confocal analysis, we demonstrated that PARP-14 is activated after cytokine treatment in α and β cells. A possible link between PARP-14 and interleukin was described (15). In this paper, they demonstrated that IL-4 protection of B cells from apoptosis depends on PARP-14. In our model, treatment of the two cell types with cytokines caused cell death only of β TC1 cells. β cell loss is traditionally considered a major cause of type I diabetes onset. On the other hand, a concomitant role of glucagon secreting pancreatic α cells in the pathogenesis of type I diabetes has been proposed (46–48). As is well-documented, both α and β cells have a common origin, but the latter are more vulnerable to apoptosis under inflammatory conditions, which are common in type I diabetes (20). In this report, the authors suggested that JNK1 is a key mediator of IL-1 β -induced apoptosis in a rat β -cell line and that it is able to modulate apoptosis through the transcription factor Myc. Another study demonstrated that the use of JNK

inhibitor prevents human β cells from apoptosis, induced by glucose and leptins through the activation of JNK (49). Therefore, since PARP-14 is involved in a transduction pathway mediated by JNKs, promoting survival in multiple myeloma (16), we hypothesized the activation of this signaling pathway also in our α TC1.6 cell line, in an inflammatory experimental model. Indeed, the activation of this protective pathway could explain the resistance of α cells to apoptosis induced by cytokines. For this reason, since β cells are more vulnerable to an inflammatory environment and express lower levels of PARP-14 than α cells, we considered β cells a useful comparison system. Our results deepen our knowledge regarding the role played by JNKs and PARP-14 in pancreatic α TC1.6 and in β TC1 cells, in an inflammatory state. In particular, JNK1 expression levels showed a different behavior in α TC1.6 compared to β TC1 cells. In fact, in α TC1.6 cells, the inflammatory state did not determine any significant increase in JNK1 expression, proving that cytokines were not able to trigger the apoptotic cascade mediated by this protein. Conversely, in the same conditions, β TC1 cells up-regulate JNK1 expression and p53 phosphorylation mediated by JNK1, thus activating apoptosis. Furthermore, at 48 h, under inflammatory conditions and in the presence of PJ-34, α cells overexpressed JNK1, responsible for p53 phosphorylation. These data show that, when PARP-14 is inhibited, the role played by JNK1 in inducing apoptosis prevails. In addition, the ability of PJ-34 to

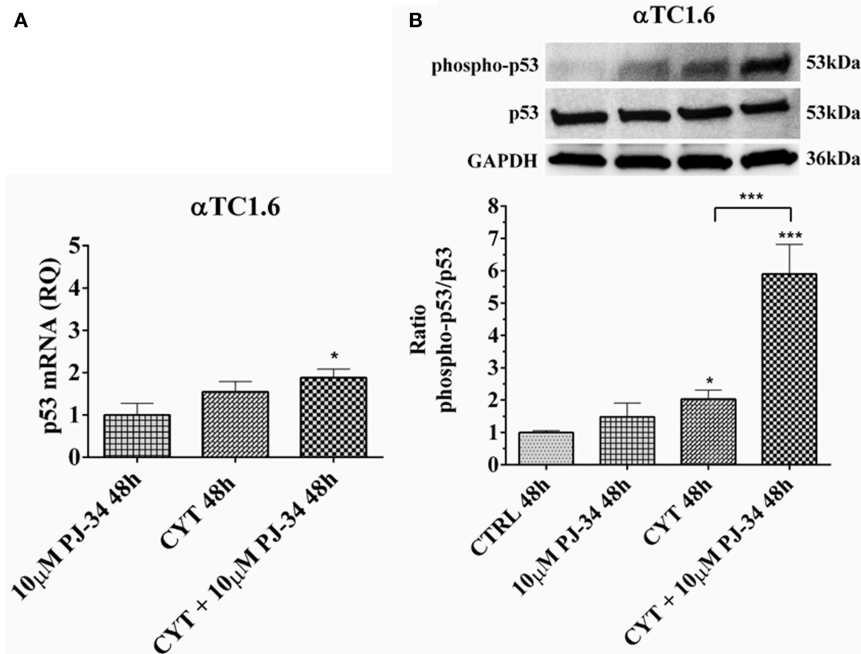


FIGURE 11 | Effect of the PARP inhibitor PJ-34 on p53 mRNA expression and p53 phosphorylation level in α TC1.6 cells, grown for 48 h in the presence or absence of cytokines. Real-time PCR and total cell lysate immunoblottings were performed as described in the Materials and Methods section. α TC1.6 cells were grown: in normal culture medium (control: CTRL); in the presence of 10 μ M PJ-34; in culture medium containing cytokine cocktail (CYT: TNF- α 25 U/ml; IFN- γ 25 U/ml and IL-1 β 0.1 U/ml); in culture medium with the addition of both cytokine cocktail and 10 μ M PJ-34 (CYT + 10 μ M PJ-34), for 48 h. **(A)** Relative quantity (RQ) level of p53 mRNA, at 48 h, in the experimental conditions mentioned above. Relative quantification is referred to untreated cells. **(B)** The phosphorylation level of p53 protein was revealed with a rabbit polyclonal antibody (1:1000 dilution) as described in Materials and Methods section. The phosphorylated form of p53 was normalized with the total protein, using a mouse monoclonal antibody (1:1000 dilution). The blots were controlled for equal loading by GAPDH, using a mouse monoclonal antibody (1:2000 dilution). Immunoreactive bands were visualized by chemiluminescence (ECL system). The values were obtained by the reading of blots through the Image J program. Statistical analysis was carried out by One-way Anova test, using control (CTRL) and cytokines (CYT) conditions as reference samples. The bars represent means \pm SD of three independent experiments (S.D. = standard deviation). Asterisks represent a significant difference between the condition and CTRL. The significance between CYT + 10 μ M PJ-34 and CYT is indicated by the asterisks upon the sticks (*** p < 0.001; * p < 0.05).

make α TC1.6 cells susceptible to apoptotic death induction by cytokines was confirmed by flow cytometry. In fact, the reduction of vital cells and the concomitant increase of early apoptotic cell populations were found only in the presence of PJ-34. On the contrary, in β cells, the reduction of early apoptotic cell rate was followed by an increase of the late apoptotic cell rate, indicating that β cells go to an irreversible apoptotic cell death. These results are consistent with the expression levels of JNK1. Moreover, the addition of PJ-34 reduced JNK1 expression and p53 phosphorylation, only at 24 h. However, since the reduction of these proteins was not followed by an increase of β cell survival (see flow cytometry results), we could hypothesize that, unlike α cells, β cell death might not be dependent only on the JNK1-p53 pathway. On the other hand, further studies are needed to investigate the role played by PARP inhibitor PJ-34 and these two pro-apoptotic proteins in the β TC1 cell line. Further proof of the protective role of PARP-14 as well as the absence of susceptibility of α TC1.6 cells to apoptotic death, induced by inflammation, was provided by the caspase-3 activity assay. As was reported, PARP-14 promotes survival by inhibiting caspase activity (17). It was demonstrated that IL-4 is less efficient in reducing caspase activity in PARP-14 KO

B cells. Therefore, in our model, cytokine stimulation, in α cells, was not able to induce any variation of caspase-3 activity at both time points, demonstrating, once again, the resistance of this cell line to inflammatory insults. In fact, the increase of caspase-3 catalytic ability, in α cell, occurred only at 48 h, when PARP-14 is blocked by PJ-34. In this case, the caspase-3 catalytic activity variation is due to PARP-14 inhibition by PJ-34 and not to cytokine stimulation. Instead, β cells appear to be susceptible to the action of cytokines, as demonstrated by the increase of caspase-3 activity levels, which were maintained after the addition of PJ-34. It seems clear that, in these cells, PJ-34 did not affect caspase-3 activity, proving that it acts in a different way than in α TC1.6 cells. Finally, through the expression patterns of JNK2 and PARP-14, we demonstrated that the resistance of α cells to an inflammatory environment is due to the activation of the JNK2/PARP-14 survival pathway. The mRNA trend and confocal analysis showed that α TC1.6 cells overexpressed PARP-14 only when they were stimulated by cytokines, mainly at 48 h. However, at this time point, the addition of the PARP inhibitor PJ-34 was able to counteract the increase of PARP-14 expression, induced by cytokines. At 48 h, the inflammatory state also caused a significant increment of JNK2 expression that

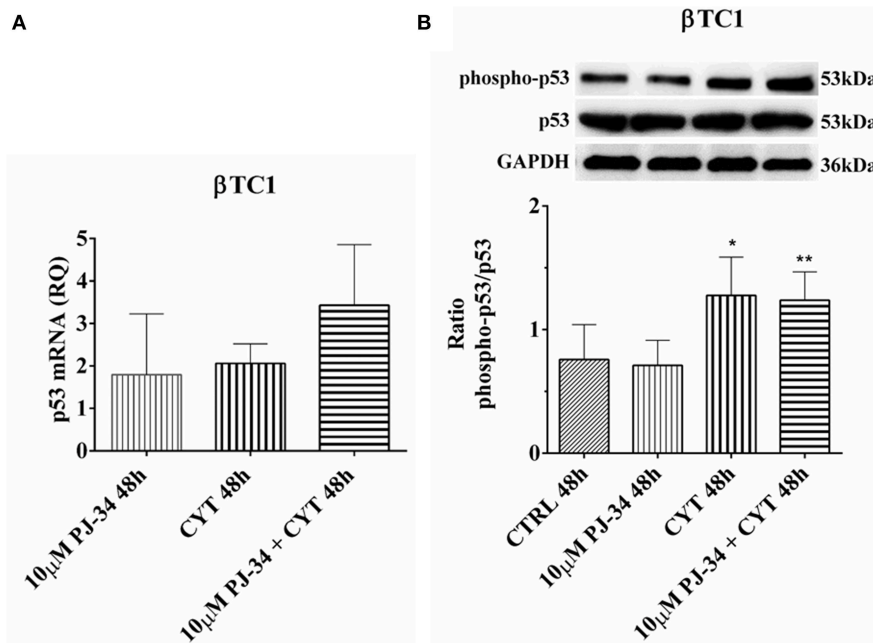


FIGURE 12 | Effect of the PARP inhibitor PJ-34 on p53 mRNA expression and p53 phosphorylation level in βTC1 cells, grown for 48 h in the presence or absence of cytokines. Real-time PCR and total cell lysate immunoblottings were performed as described in the Materials and Methods section. βTC1 cells were grown: in normal culture medium (control: CTRL); in the presence of 10 μM PJ-34; in culture medium containing cytokine cocktail (CYT: TNF-α 25 U/ml; IFN-γ 25 U/ml and IL-1β 0.1 U/ml); in culture medium with the addition of both cytokine cocktail and 10 μM PJ-34 (CYT + 10 μM PJ-34), for 48 h. **(A)** Relative quantity (RQ) level of p53 mRNA, at 48 h, in the experimental conditions mentioned above. Relative quantification is referred to untreated cells. **(B)** The phosphorylation level of p53 protein was revealed with a rabbit polyclonal antibody (1:1000 dilution) as described in Materials and Methods section. The phosphorylated form of p53 was normalized with the total protein, using a mouse monoclonal antibody against total p53 (1:1000 dilution). The blots were controlled for equal loading by GAPDH, using a mouse monoclonal antibody (1:2000 dilution). Immunoreactive bands were visualized by chemiluminescence (ECL system). The values were obtained by the reading of blots through the Image J program. Statistical analysis was carried out by One-way Anova test, using control (CTRL) and cytokines (CYT) conditions as reference samples. The bars represent means ± SD of three independent experiments (S.D. = standard deviation). Asterisks represent a significant difference between the condition and CTRL (** $p < 0.01$; * $p < 0.05$).

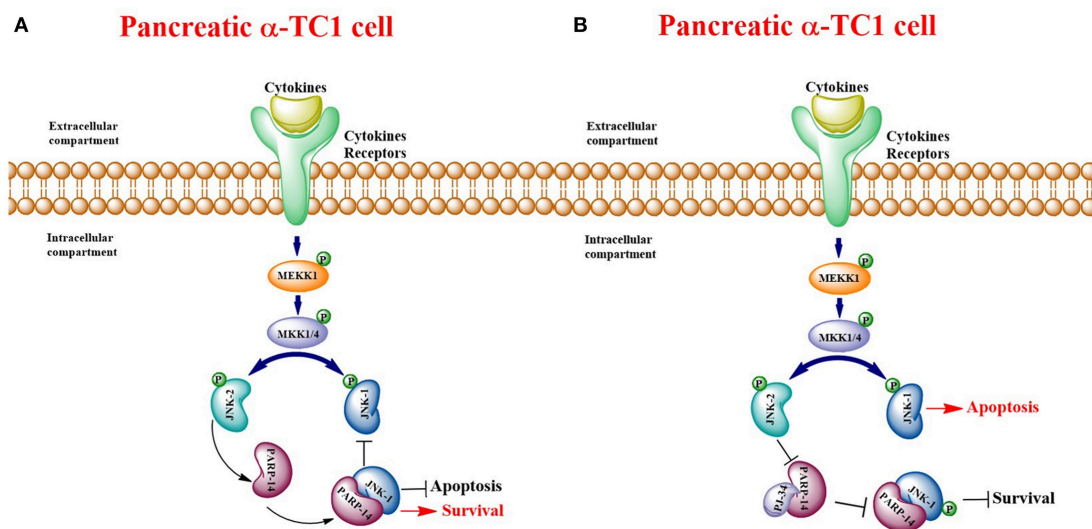


FIGURE 13 | Schematic model of pancreatic αTC1.6 cells pathways. Binding of cytokines to their specific receptors activates the Mitogen-Activated Protein Kinase (MAPK) signaling cascade: this culminates in the activation of the Stress-Activated Protein Kinases (SAPK)/c Jun N-terminal Kinases (JNK). Therefore, in presence of inflammatory stimuli, JNK-2 activates PARP-14, which binds to and counteracts the pro-apoptotic protein JNK-1, promoting cell survival **(A)**. PARP-14, bound to the inhibitor PJ-34, is not able to interact with other molecules and JNK-1 can trigger apoptotic death **(B)**.

was higher in the presence of PJ-34. Briefly, when PARP-14 is blocked, JNK2 is further up-regulated, favoring the beginning of the survival signaling cascade. Instead, the down-regulation of JNK2 mediated by PJ-34 at 24 h could indicate that, at this time point, the inflammatory stimulation is not adequate to trigger a survival pathway, as was demonstrated by flow cytometry. In β cells, the trend of PARP-14 and JNK2 clearly confirms that this signaling cascade was not engaged. All these data, taken together, demonstrate that PARP-14 is definitely involved in the resistance of pancreatic α cells to inflammatory insults, through the transduction pathway mediated by JNK proteins promoting survival or apoptosis. In this regard, we hypothesized that the interaction between PARP-14 and its inhibitor could impede the protein binding JNK1, which should be free to trigger the apoptosis cascade (see schematic model in **Figure 13**). Certainly, further work will be required to elucidate other mechanisms involved in this complex signal transduction pathway.

CONCLUSION

This study must be seen as a first piece of a puzzle where PARP-14, JNKs and PJ-34 play key roles in the pancreatic microenvironment and provide starting points from which to explore further.

AUTHOR CONTRIBUTIONS

VS-P conceived the project and designed the experiments together with MP and CD. MR and FD performed molecular

experiments as RT-PCR and western analysis. CS and MS performed confocal analysis. FD, NM, and VB performed cytofluorimetric analysis. FD and MC were in charge of cell culture and treatment. FD performed computational and statistical data analysis, together with AT-S. VS-P and FD wrote the paper. All authors contributed to the critical revision of the data, read and approved the final manuscript.

FUNDING

This work was supported by *Ricerca di Ateneo* grant, University of Catania.

ACKNOWLEDGMENTS

The authors acknowledge the PON project Bio-nanotech Research and Innovation Tower (BRIT), financed by the Italian Ministry for Education, University and Research (MIUR) (Grant no. PONa3_00136).

We are thankful also to Giorgia Spampinato and Irina Naletova for expert technical assistance.

Finally, we thank the Scientific Bureau of the University of Catania for language support.

SUPPLEMENTARY MATERIAL

The Supplementary Material for this article can be found online at: <https://www.frontiersin.org/articles/10.3389/fendo.2019.00271/full#supplementary-material>

REFERENCES

- Ba X, Garg NJ. Signaling mechanism of poly(ADP-ribose) polymerase-1 (PARP-1) in inflammatory diseases. *Am J Pathol.* (2011) 178:946–55. doi: 10.1016/j.ajpath.2010.12.004
- Matveeva E, Maiorano J, Zhang Q, Eteleeb AM, Convertini P, Chen J, et al. Involvement of PARP1 in the regulation of alternative splicing. *Cell Discov.* (2016) 2:15046. doi: 10.1038/celldisc.2015.46
- Sethi GS, Dharwal V, Naura AS. Poly(ADP-Ribose)polymerase-1 in lung inflammatory disorders: a review. *Front Immunol.* (2017) 8:1172. doi: 10.3389/fimmu.2017.01172
- Spina-Purrello V, Patti D, Giuffrida-Stella AM, Nicoletti VG. Parp and cell death or protection in rat primary astroglial cell cultures under LPS/IFN γ induced proinflammatory conditions. *Neurochem Res.* (2008) 33:2583–92. doi: 10.1007/s11064-008-9835-1
- Vyas S, Chang P. New PARP targets for cancer therapy. *Nat Rev Cancer.* (2014) 14:502–9. doi: 10.1038/nrc3748
- Ame JC, Spenlehauer C, de Murcia G. The PARP superfamily. *Bioessays.* (2004) 26:882–93. doi: 10.1002/bies.20085
- D'Amours D, Desnoyers S, D'Silva I, Poirier GG. Poly(ADP-ribosylation) reactions in the regulation of nuclear functions. *Biochem. J.* (1999) 342(Pt. 2):249–68.
- Gupte R, Liu Z, Kraus WL. PARPs and ADP-ribosylation: recent advances linking molecular functions to biological outcomes. *Genes Dev.* (2017) 31:101–26. doi: 10.1101/gad.291518.116
- Hassa PO, Hottiger MO. The diverse biological roles of mammalian PARPs, a small but powerful family of poly-ADP-ribose polymerases. *Front Biosci.* (2008) 13:3046–82. doi: 10.2741/2909
- Hottiger MO, Hassa PO, Luscher B, Schuler H, Koch-Nolte F. Toward a unified nomenclature for mammalian ADP-ribosyltransferases. *Trends Biochem Sci.* (2010) 35:208–19. doi: 10.1016/j.tibs.2009.12.003
- Vyas S, Chesaronne-Cataldo M, Todorova T, Huang YH, Chang P. A systematic analysis of the PARP protein family identifies new functions critical for cell physiology. *Nat Commun.* (2013) 4:2240. doi: 10.1038/ncomms3240
- Gibson BA, Kraus WL. New insights into the molecular and cellular functions of poly(ADP-ribose) and PARPs. *Nat Rev Mol Cell Biol.* (2012) 13:411–24. doi: 10.1038/nrm3376
- Vyas S, Matic I, Uchima L, Rood J, Zaja R, Hay RT, et al. Family-wide analysis of poly(ADP-ribose) polymerase activity. *Nat Commun.* (2014) 5:4426. doi: 10.1038/ncomms5426
- Underhill C, Toulmonde M, Bonnefoi H. A review of PARP inhibitors: from bench to bedside. *Ann Oncol.* (2011) 22:268–79. doi: 10.1093/annonc/mdq322
- Cho SH, Ahn AK, Bhargava P, Lee CH, Eischen CM, McGuinness O, et al. Glycolytic rate and lymphomagenesis depend on PARP14, an ADP ribosyltransferase of the B aggressive lymphoma (BAL) family. *Proc Natl Acad Sci USA.* (2011) 108:15972–7. doi: 10.1073/pnas.1017082108
- Barbarulo A, Iansante V, Chaidos A, Naresh K, Rahemtulla A, Franzoso G, et al. Poly(ADP-ribose) polymerase family member 14 (PARP14) is a novel effector of the JNK2-dependent pro-survival signal in multiple myeloma. *Oncogene.* (2013) 32:4231–42. doi: 10.1038/onc.2012.448
- Cho SH, Goenka S, Henttinen T, Gudapati P, Reinikainen A, Eischen CM, et al. PARP-14, a member of the B aggressive lymphoma family, transduces survival signals in primary B cells. *Blood.* (2009) 113:2416–25. doi: 10.1182/blood-2008-03-144121
- Mehrotra P, Riley JR, Patel R, Li F, Voss L, Goenka S. PARP-14 functions as a transcriptional switch for Stat6-dependent gene activation. *J Biol Chem.* (2011) 286:1767–76. doi: 10.1074/jbc.M110.157768

19. Mehrotra P, Hollenbeck A, Riley JP, Li F, Patel RJ, Akhtar N, et al. Poly (ADP-ribose) polymerase 14 and its enzyme activity regulates T(H)2 differentiation and allergic airway disease. *J Allergy Clin Immunol.* (2013) 131:521–31 e1–12. doi: 10.1016/j.jaci.2012.06.015
20. Prause M, Berchtold LA, Urizar AI, Hyldgaard Trauelsen M, Billestrup N, Mandrup-Poulsen T, et al. TRAF2 mediates JNK and STAT3 activation in response to IL-1beta and IFNgamma and facilitates apoptotic death of insulin-producing beta-cells. *Mol Cell Endocrinol.* (2016) 420:24–36. doi: 10.1016/j.mce.2015.11.021
21. Bubici C, Papa S. JNK signalling in cancer: in need of new, smarter therapeutic targets. *Br J Pharmacol.* (2014) 171:24–37. doi: 10.1111/bph.12432
22. Barbagallo D, Piro S, Condorelli AG, Mascali LG, Urbano F, Parrinello N, et al. miR-296-3p, miR-298-5p and their downstream networks are causally involved in the higher resistance of mammalian pancreatic alpha cells to cytokine-induced apoptosis as compared to beta cells. *BMC Genomics.* (2013) 14:62. doi: 10.1186/1471-2164-14-62
23. Barbagallo D, Condorelli AG, Piro S, Parrinello N, Floyel T, Ragusa M, et al. CEBPA exerts a specific and biologically important proapoptotic role in pancreatic beta cells through its downstream network targets. *Mol Biol Cell.* (2014) 25:2333–41. doi: 10.1091/mbc.E14-02-0703
24. Eizirik DL, Colli ML, Ortis F. The role of inflammation in insulinitis and beta-cell loss in type 1 diabetes. *Nat Rev Endocrinol.* (2009) 5:219–26. doi: 10.1038/nrendo.2009.21
25. Mathis D, Vence L, Benoist C. beta-Cell death during progression to diabetes. *Nature.* (2001) 414:792–8. doi: 10.1038/414792a
26. Di Pietro C, Vento M, Guglielmino MR, Borzi P, Santonocito M, Ragusa M, et al. Molecular profiling of human oocytes after vitrification strongly suggests that they are biologically comparable with freshly isolated gametes. *Fertil Steril.* (2010) 94:2804–7. doi: 10.1016/j.fertnstert.2010.04.060
27. Scalia M, Satriano C, Greca R, Stella AM, Rizzarelli E, Spina-Purrello V. PARP-1 inhibitors DPQ and PJ-34 negatively modulate proinflammatory commitment of human glioblastoma cells. *Neurochem Res.* (2013) 38:50–8. doi: 10.1007/s11064-012-0887-x
28. Cardullo N, Pulvirenti L, Spatafora C, Musso N, Barresi V, Condorelli DF, et al. Dihydrobenzofuran neolignanamides: laccase-mediated biomimetic synthesis and antiproliferative activity. *J Nat Prod.* (2016) 79:2122–34. doi: 10.1021/acs.jnatprod.6b00577
29. Anfuso CD, Lupo G, Romeo L, Giurdanella G, Motta C, Pascale A, et al. Endothelial cell-pericyte cocultures induce PLA2 protein expression through activation of PKCalpha and the MAPK/ERK cascade. *J Lipid Res.* (2007) 48:782–93. doi: 10.1194/jlr.M600489-JLR200
30. Lupo G, Nicotra A, Giurdanella G, Anfuso CD, Romeo L, Biondi G, et al. Activation of phospholipase A(2) and MAP kinases by oxidized low-density lipoproteins in immortalized GP8.39 endothelial cells. *Biochim Biophys Acta.* (2005) 1735:135–50. doi: 10.1016/j.bbali.2005.05.008
31. Burkle A. Physiology and pathophysiology of poly(ADP-ribosyl)ation. *Bioessays.* (2001) 23:795–806. doi: 10.1002/bies.1115
32. Gibson BA, Zhang Y, Jiang H, Hussey KM, Shrimp JH, Lin H, et al. Chemical genetic discovery of PARP targets reveals a role for PARP-1 in transcription elongation. *Science.* (2016) 353:45–50. doi: 10.1126/science.aaf7865
33. Krishnakumar R, Kraus WL. PARP-1 regulates chromatin structure and transcription through a KDM5B-dependent pathway. *Mol Cell.* (2010) 39:736–49. doi: 10.1016/j.molcel.2010.08.014
34. Vilar E, Bartnik CM, Stenzel SL, Raskin L, Ahn J, Moreno V, et al. MRE11 deficiency increases sensitivity to poly(ADP-ribose) polymerase inhibition in microsatellite unstable colorectal cancers. *Cancer Res.* (2011) 71:2632–42. doi: 10.1158/0008-5472.CAN-10-1120
35. Motta C, D'Angeli F, Scalia M, Satriano C, Barbagallo D, Naletova I, et al. PJ-34 inhibits PARP-1 expression and ERK phosphorylation in glioma-conditioned brain microvascular endothelial cells. *Eur J Pharmacol.* (2015) 761:55–64. doi: 10.1016/j.ejphar.2015.04.026
36. Weaver AN, Yang ES. Beyond DNA repair: additional functions of PARP-1 in cancer. *Front Oncol.* (2013) 3:290. doi: 10.3389/fonc.2013.00290
37. Bai XT, Moles R, Chaib-Mezrag H, Nicot C. Small PARP inhibitor PJ-34 induces cell cycle arrest and apoptosis of adult T-cell leukemia cells. *J Hematol Oncol.* (2015) 8:117. doi: 10.1186/s13045-015-0217-2
38. Lavarone E, Puppini C, Passon N, Filetti S, Russo D, Damante G. The PARP inhibitor PJ34 modifies proliferation, NIS expression and epigenetic marks in thyroid cancer cell lines. *Mol Cell Endocrinol.* (2013) 365:1–10. doi: 10.1016/j.mce.2012.08.019
39. McCann KE, Hurvitz SA. Advances in the use of PARP inhibitor therapy for breast cancer. *Drugs Context.* (2018) 8:212540. doi: 10.7573/dic.212540
40. Steffen JD, Brody JR, Armen RS, Pascal JM. Structural implications for selective targeting of PARPs. *Front Oncol.* (2013) 3:301. doi: 10.3389/fonc.2013.00301
41. Tentori L, Ricci-Vitiani L, Muzi A, Ciccarone F, Pelacchi F, Calabrese R, et al. Pharmacological inhibition of poly(ADP-ribose) polymerase-1 modulates resistance of human glioblastoma stem cells to temozolomide. *BMC Cancer.* (2014) 14:151. doi: 10.1186/1471-2407-14-151
42. Zha S, Li Z, Cao Q, Wang F, Liu F. PARP1 inhibitor (PJ34) improves the function of aging-induced endothelial progenitor cells by preserving intracellular NAD(+) levels and increasing SIRT1 activity. *Stem Cell Res Ther.* (2018) 9:224. doi: 10.1186/s13287-018-0961-7
43. Zha S, Li Z, Cao Q, Wang F, Liu F. Correction to: PARP1 inhibitor (PJ34) improves the function of aging-induced endothelial progenitor cells by preserving intracellular NAD(+) levels and increasing SIRT1 activity. *Stem Cell Res Ther.* (2018) 9:269. doi: 10.1186/s13287-018-1019-6
44. Mehrotra P, Krishnamurthy P, Sun J, Goenka S, Kaplan MH. Poly-ADP-ribosyl polymerase-14 promotes T helper 17 and follicular T helper development. *Immunology.* (2015) 146:537–46. doi: 10.1111/imm.12515
45. Iansante V, Choy PM, Fung SW, Liu Y, Chai JG, Dyson J, et al. PARP14 promotes the Warburg effect in hepatocellular carcinoma by inhibiting JNK1-dependent PKM2 phosphorylation and activation. *Nat Commun.* (2015) 6:7882. doi: 10.1038/ncomms8882
46. Cryer PE. Minireview: glucagon in the pathogenesis of hypoglycemia and hyperglycemia in diabetes. *Endocrinology.* (2012) 153:1039–48. doi: 10.1210/en.2011-1499
47. Hughes DSN, P. Alpha cell function in type 1 diabetes. *Br J Diabetes.* (2014) 14:7. doi: 10.15277/bjdv.2014.014
48. Takahashi N, Chujo D, Kajio H, Ueki K. Contribution of pancreatic alpha-cell function to insulin sensitivity and glycemic variability in patients with type 1 diabetes. *J Diabetes Invest.* (2018). doi: 10.1111/jdi.12949. [Epub ahead of print].
49. Maedler K, Schulthess FT, Bielman C, Berney T, Bonny C, Prentki M, et al. Glucose and leptin induce apoptosis in human beta-cells and impair glucose-stimulated insulin secretion through activation of c-Jun N-terminal kinases. *Faseb J.* (2008) 22:1905–13. doi: 10.1096/fj.07-101824

Conflict of Interest Statement: The authors declare that the research was conducted in the absence of any commercial or financial relationships that could be construed as a potential conflict of interest.

Copyright © 2019 D'Angeli, Scalia, Ciriigliano, Satriano, Barresi, Musso, Trovato-Salinaro, Barbagallo, Ragusa, Di Pietro, Purrello and Spina-Purrello. This is an open-access article distributed under the terms of the Creative Commons Attribution License (CC BY). The use, distribution or reproduction in other forums is permitted, provided the original author(s) and the copyright owner(s) are credited and that the original publication in this journal is cited, in accordance with accepted academic practice. No use, distribution or reproduction is permitted which does not comply with these terms.